Experimental and Numerical Investigation of Nonlinear Density Effects on Windage Loss under High-Density sCO_2

Seungkyu Lee (KAIST)
Jeong Ik Lee (KAIST)

Table of Contents

Issues in Experiment

- Radial turbine were tested at various RPM at design condition.
- While checking the steady-state turbine power, turbine outlet temperature was higher than inlet temperature over 33,000 RPM.
- Although turbine expanded ΔP = 720kPa at design point, outlet enthalpy (457 kJ/kg) was higher than inlet enthalpy (444 kJ/kg)

RPM	Turbine Inlet Temp (℃)	Turbine Outlet Temp (℃)	Turbine Inlet Pressure (bar)	Turbine Outlet Pressure (bar)
12,000	55.22	46.91	77.11	76.25
15,000	54.85	47.28	77.59	76.25
18,000	56.05	49.75	79.57	77.68
21,000	55.76	51.34	81.00	78.47
24,000	56.53	52.95	82.00	78.66
27,000	57.93	55.50	83.84	79.65
28,000	58.13	56.24	84.37	79.85
29,000	57.68	56.18	84.38	79.53
30,000	57.90	56.81	84.95	79.78
31,000	58.39	57.73	85.59	80.09
32,000	58.36	58.13	85.98	80.17
33,000	58.92	59.10	86.71	80.56
34,000	59.63	60.24	87.52	81.01
35,000	59.44	60.39	87.90	81.07
36,000	59.07	60.32	88.16	80.97

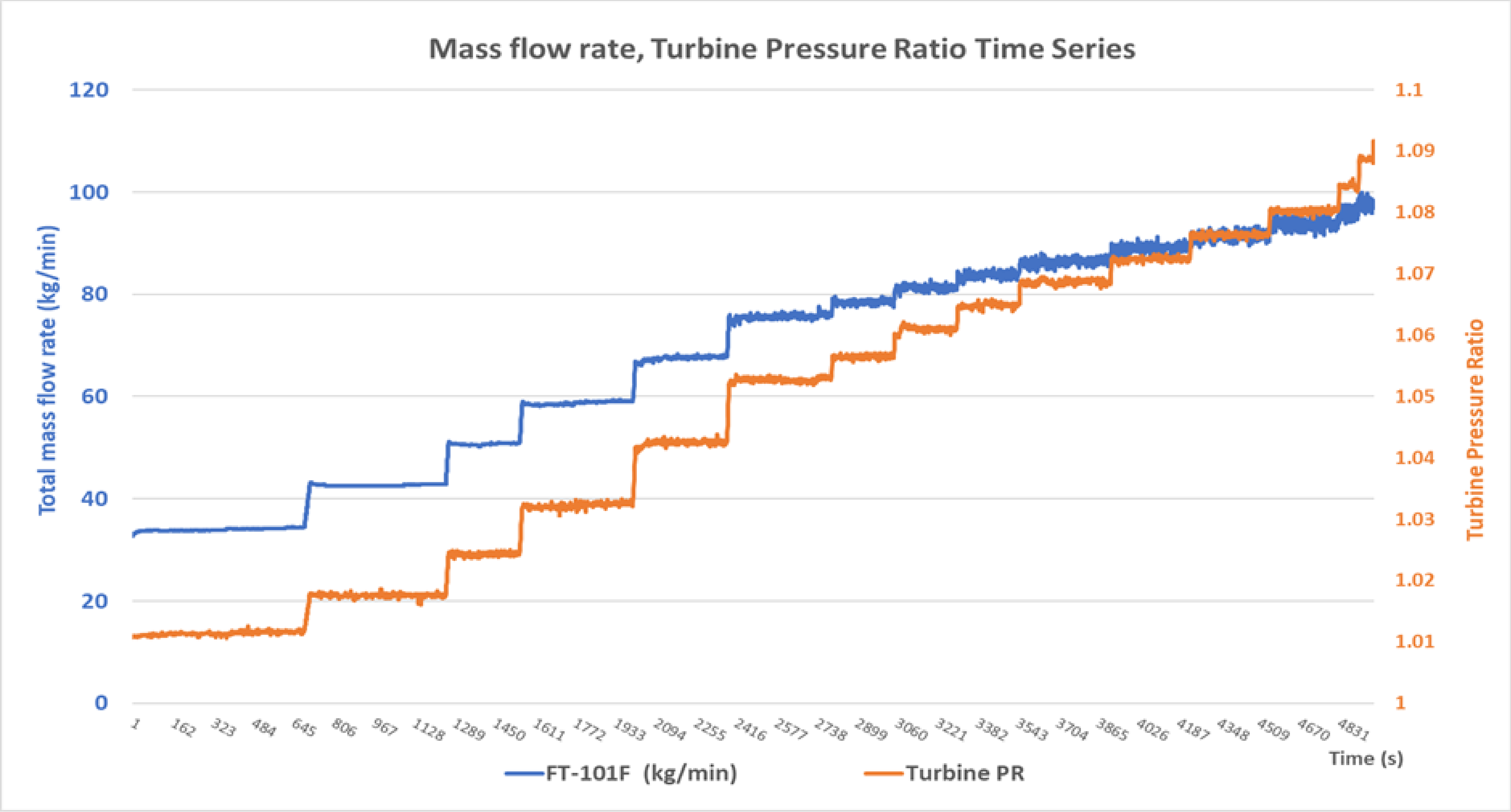

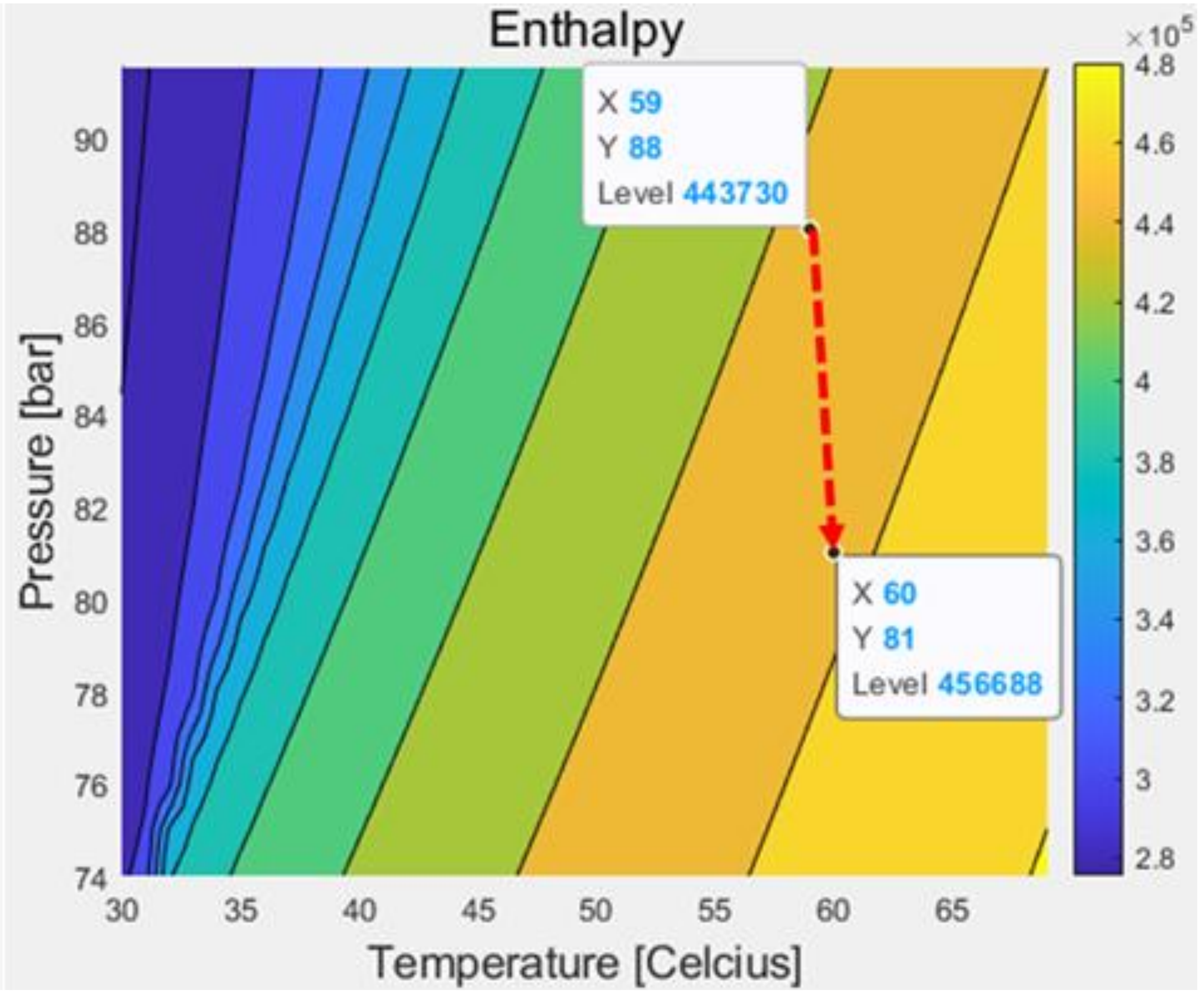

Issues in Experiment

- While checking the energy conservation at all TAC inlet & outlets, no noticeable problem was found.
- Meanwhile, 25~30% of main $\dot{m}$ flows from compressor impeller outlet to turbine rotor inlet alongside the rotor assemblies.
- High RPM (~36k) viscous heating adds the h, T of the secondary flow, and the turbine rotor inlet temperature is higher than measured temperature.

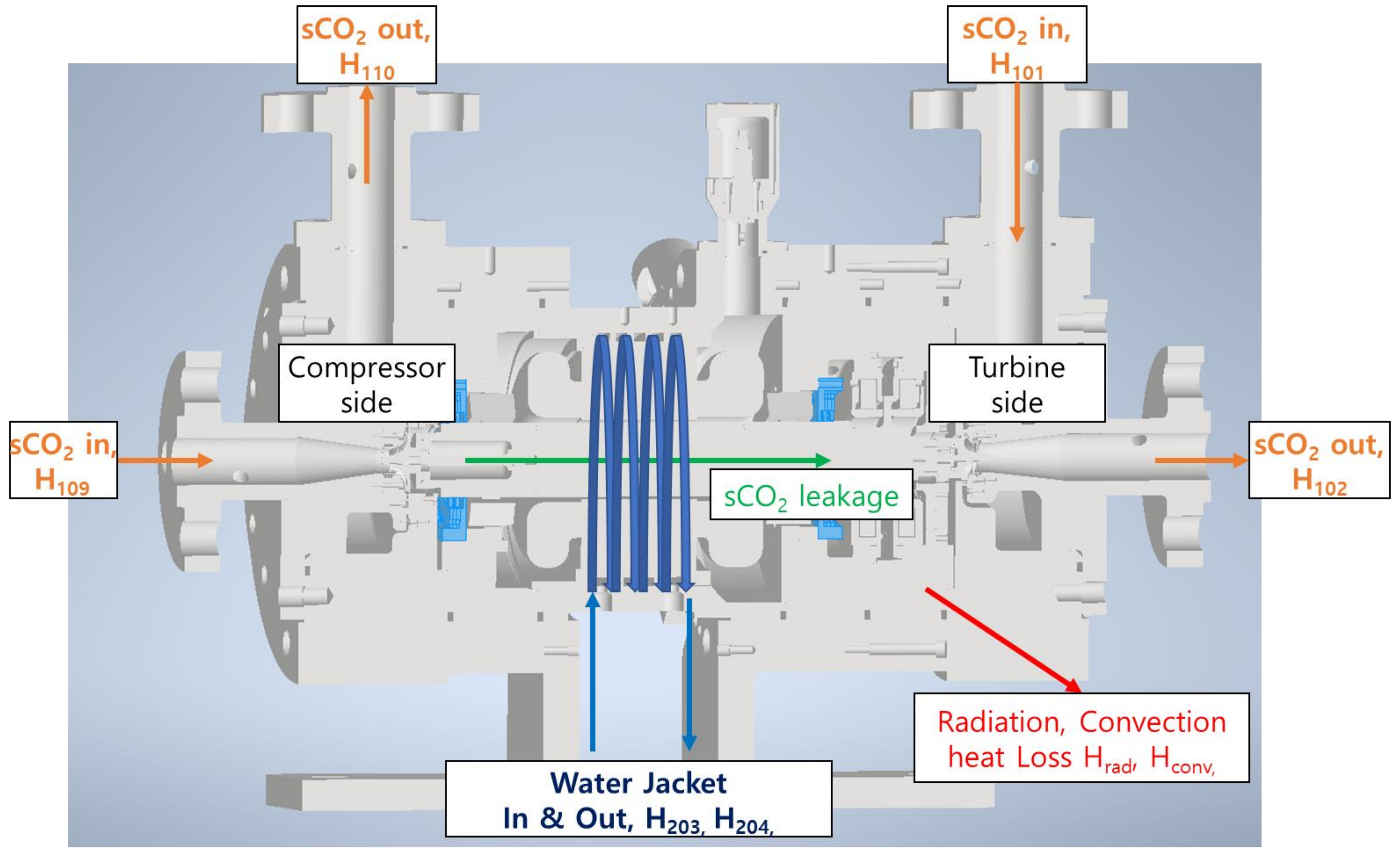

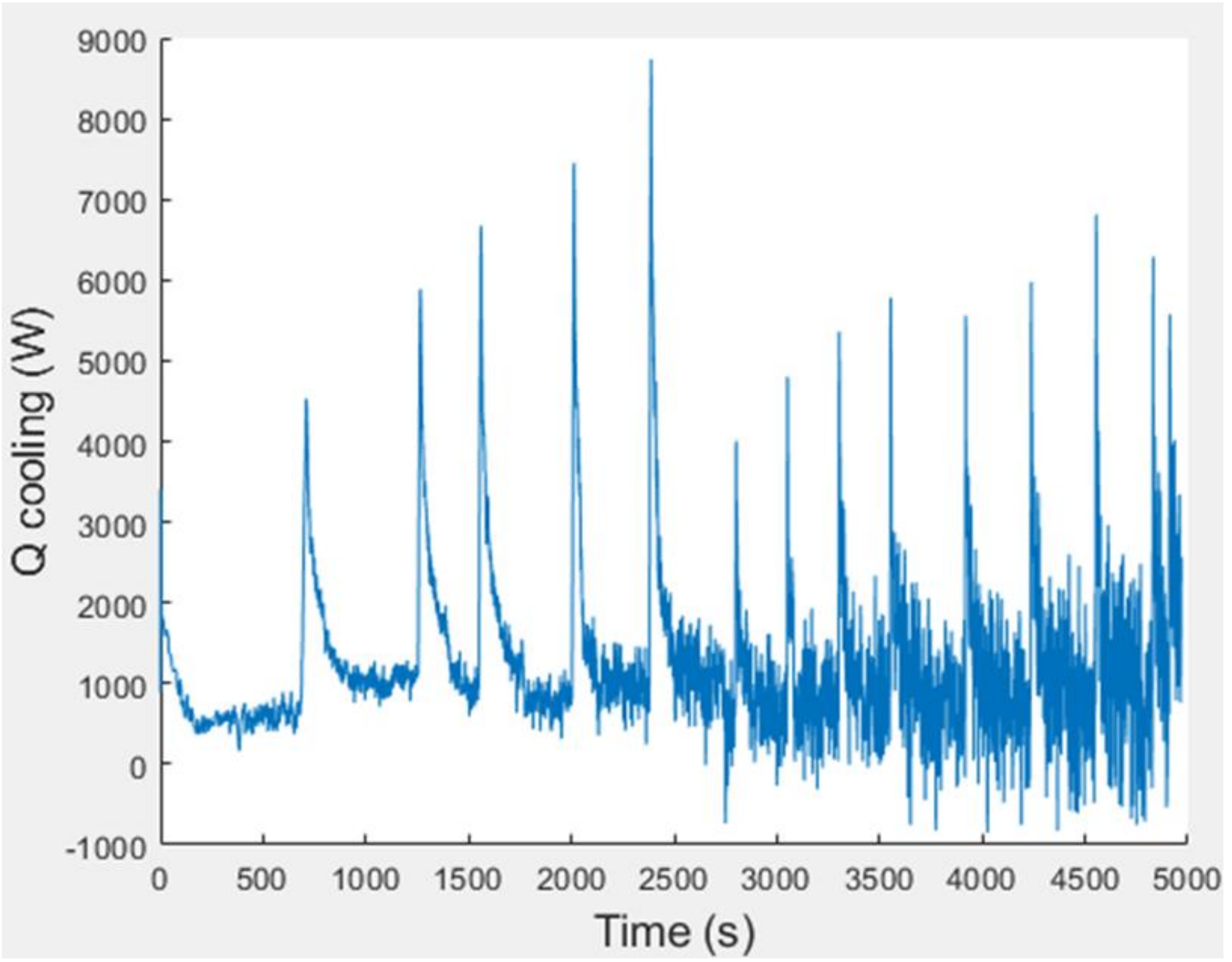

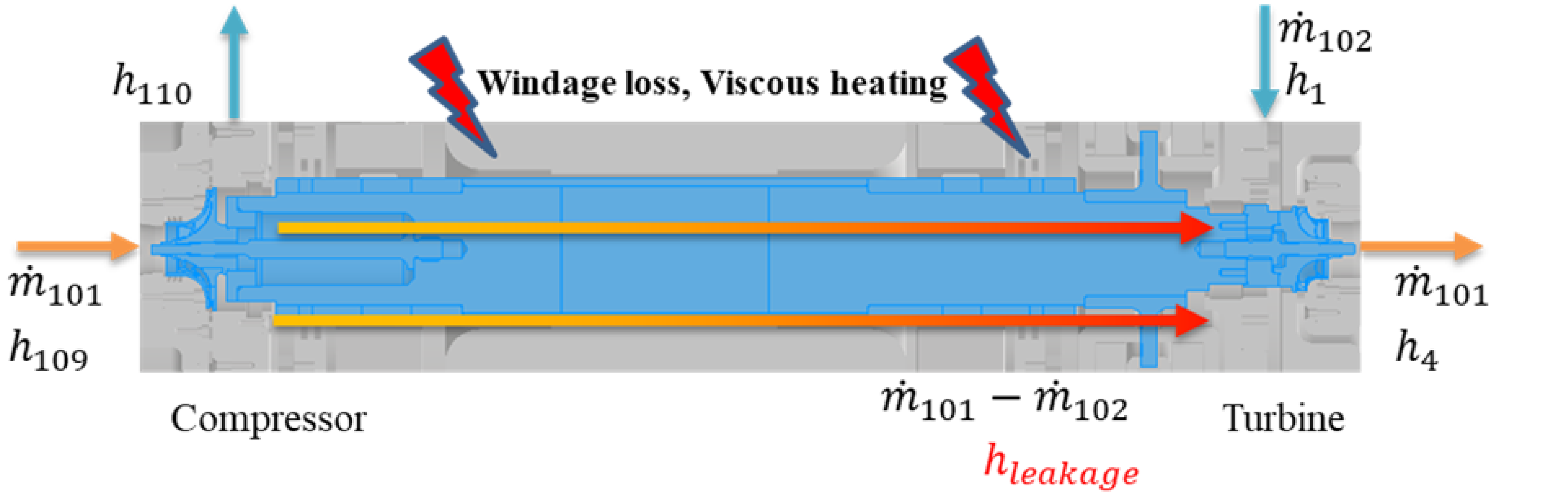

$$H_{in} = \dot{m}_{in,comp} h_{in,comp} + \dot{m}_{in,turb} h_{in,turb} + W_{motor}$$

$$H_{in} = \dot{m}_{out,comp} h_{out,comp} + \dot{m}_{out,turb} h_{out,turb}$$

$$Q_{cooling} = H_{in} - H_{out} \cong W_{windage} + H_{rad,convection}$$

High Windage Losses

- Motor power (Measured from power analyzer)
- Compressor power (Calculated from $\dot{m}_{comp}, h_{in,comp}, h_{out,comp}$)
- Turbine power (Aerodynamically max. Predicted)
  - ➢ Windage loss can be predicted from rotor power balance.

- Windage loss produced 3~5 times of the TAC compressor and Turbine power.
- Generally, sCO_2 rotor systems have high $density$ and RPM.
- For a Micro TAC rotor system, this phenomenon can have a stronger impact than expected.

➢ The windage loss correlation should be analyzed precisely.

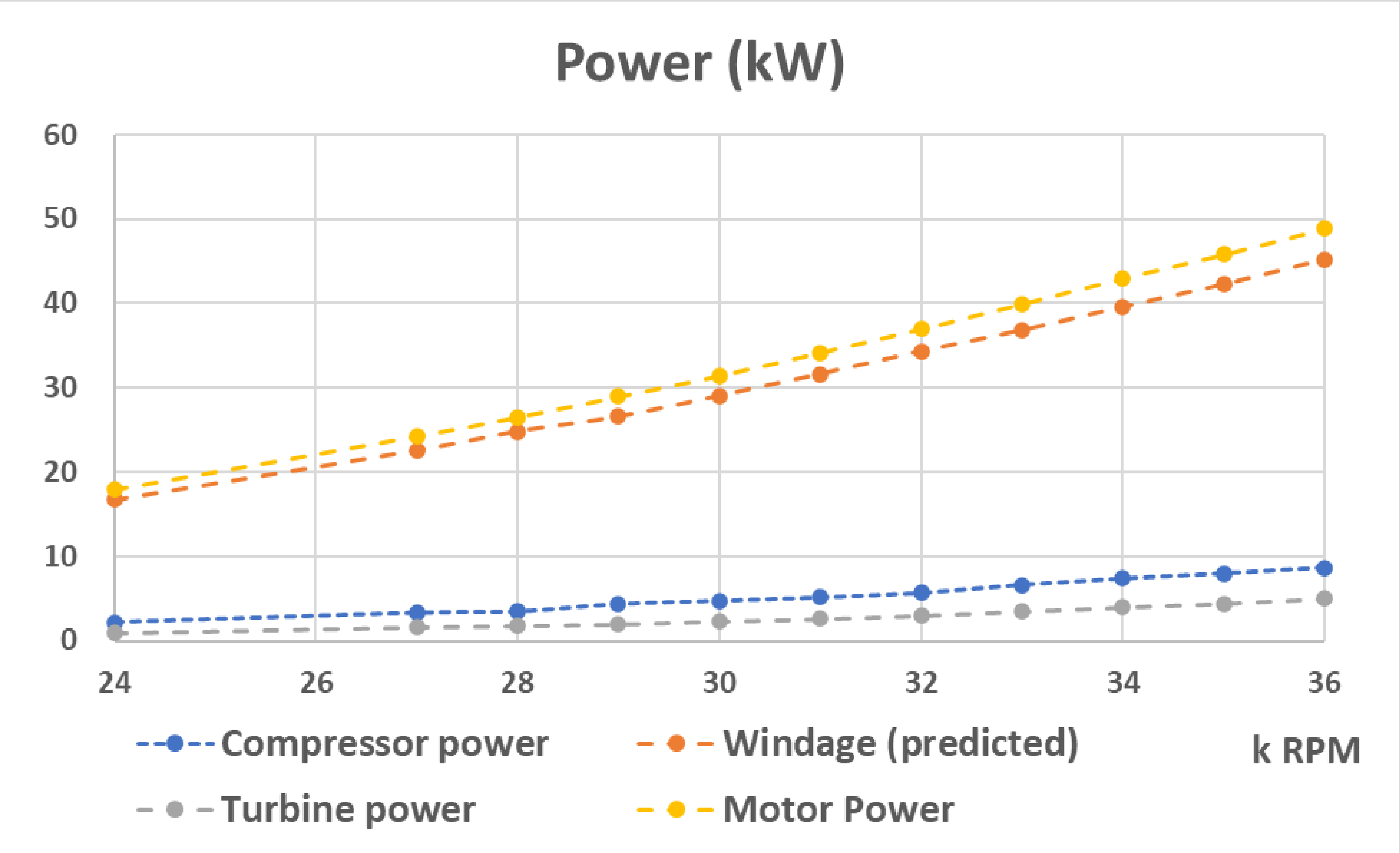

$$W_{comp} + W_{windage} = W_{turbine} + W_{motor}$$

$$W_{windage} = C_f \pi \rho R_{shaft}^4 \omega^3 L_{shaft}$$

$$W_{disk\ friction} = C_f \pi \rho (R_o^5 - R_i^5)\omega^3$$

Windage and Disk friction losses

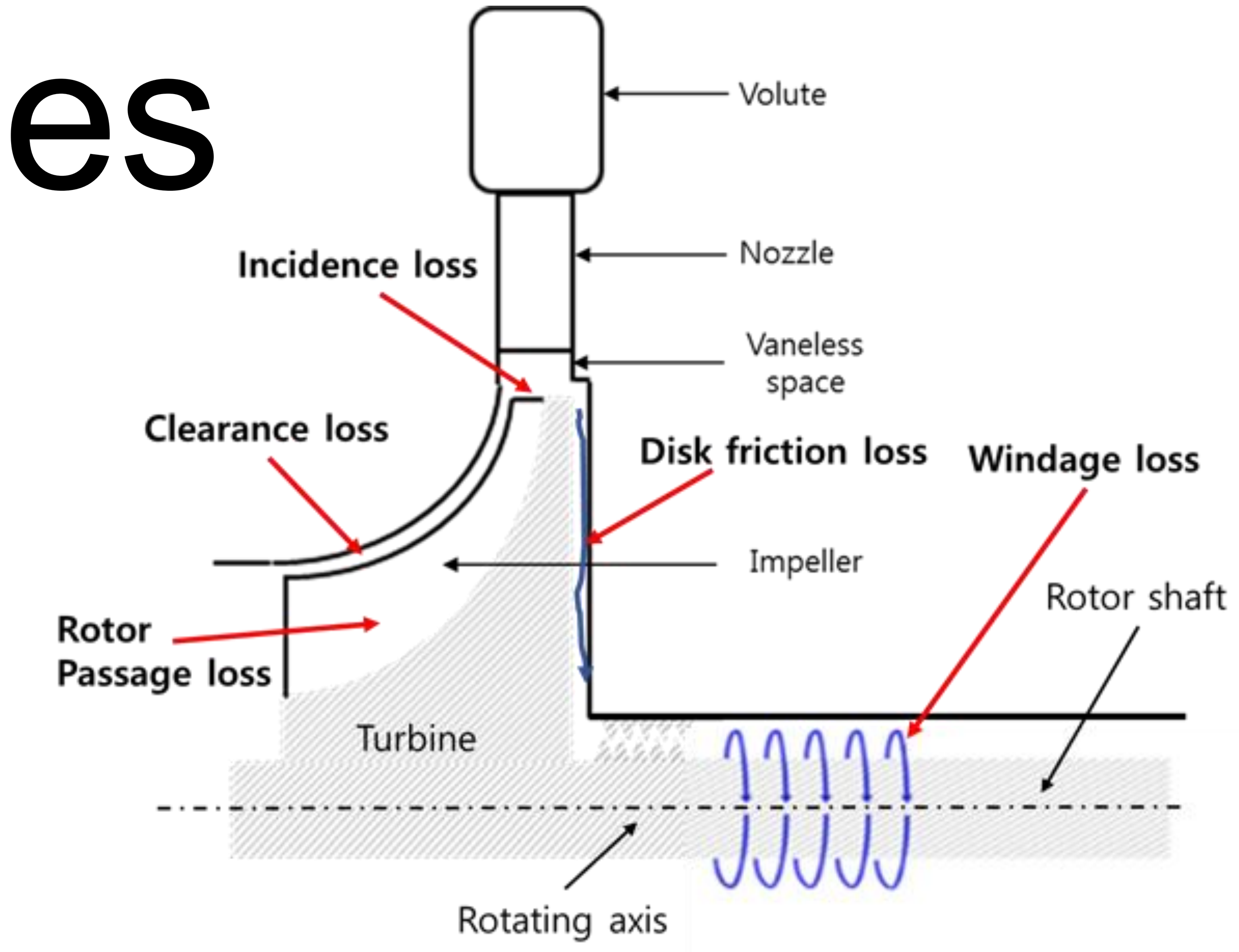

- In a rotor, disk friction occurs perpendicular to the rotational axis while the windage loss occurs parallel to the axis, fundamentally governed by same mechanism.
- According to dimensional analysis, these two losses calculated as being linearly proportional to density and proportional to the cube of rotational speed.
- However, as the Daily and Nece's disk friction correlation, coefficient (C_f) differs with the flow regimes reflecting ρ & ω effects.
- These equations show that the effects of density and rotational speed on windage loss may not be determined solely by dimensional analysis.

$$W_{windage} \sim \rho R_{shaft}^{4} \omega^{3} L_{shaft} \qquad C_f \sim \mathrm{Re}_c^{-\varepsilon} \qquad Re_c = \frac{\rho \omega R c}{\mu}$$

$$W_{disk\ friction} \sim \rho (R_o^5 - R_i^5) \omega^3$$

➢ $W_{disk\ friction} \sim \rho^{1-\varepsilon} \omega^{3-\varepsilon}$

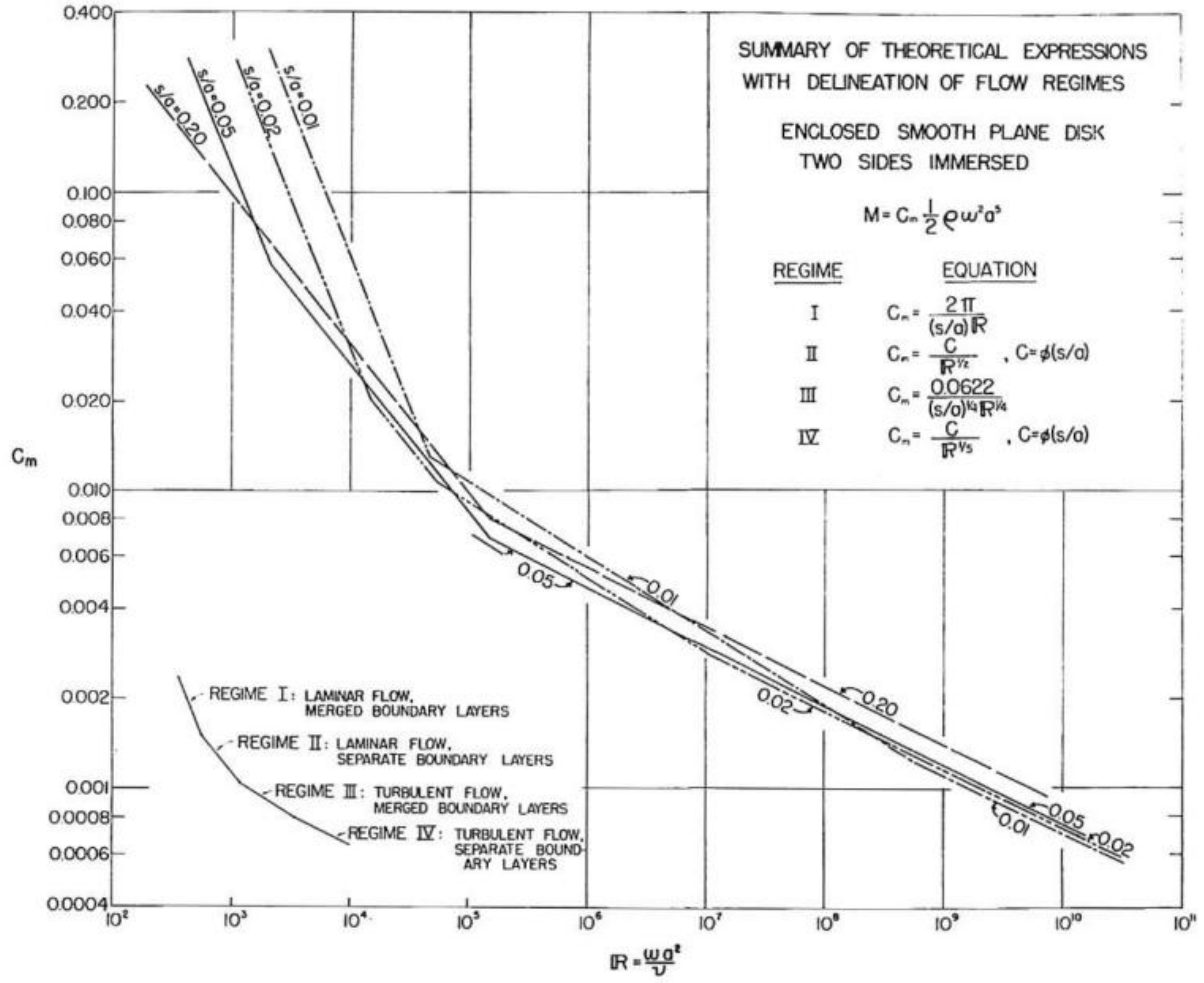

Fig. 6 Delineation of flow regimes by enclosed-disk theory

Daily, J. W., & Nece, R. E. (1960). Chamber dimension effects on induced flow and frictional resistance of enclosed rotating disks.

Original (base) Loss Models

- For the Taylor-Couette flow, laminar and turbulent regime is divided by Ta number, and $Ta_{crit} = 1700$.
- However, the KAIST-TAC Ta number is more than 10^7 due to its high density and low viscosity.
- In this study, Daily and Nece's Disk friction loss correlation is adopted.
- For the windage loss model, an expression derived from the flow–torque relationship without imposing any additional conditions was adopted.
- The coefficient is set to 0.001, which is commonly used in the turbulent regime for Re number over 10^7.

$$Ta_{windage} = 4\omega^2 R^4 \rho^2 / \mu^2$$

$$Ta_{disk} = 4\omega^2 (R_{outer}^4 - R_{inner}^4) \rho^2 / \mu^2$$

$$W_{windage} = C_f \pi \rho R_j^4 \omega^3 L_j$$

$$W_{disk\ friction} = C_f \pi \rho (R_o^5 - R_i^5) \omega^3$$

$$C_f = 0.001\ (set)$$

$$C_f = \frac{0.0622}{Re_c^{0.2}}, where\ Re_c = \frac{\rho \omega R c}{\mu}$$

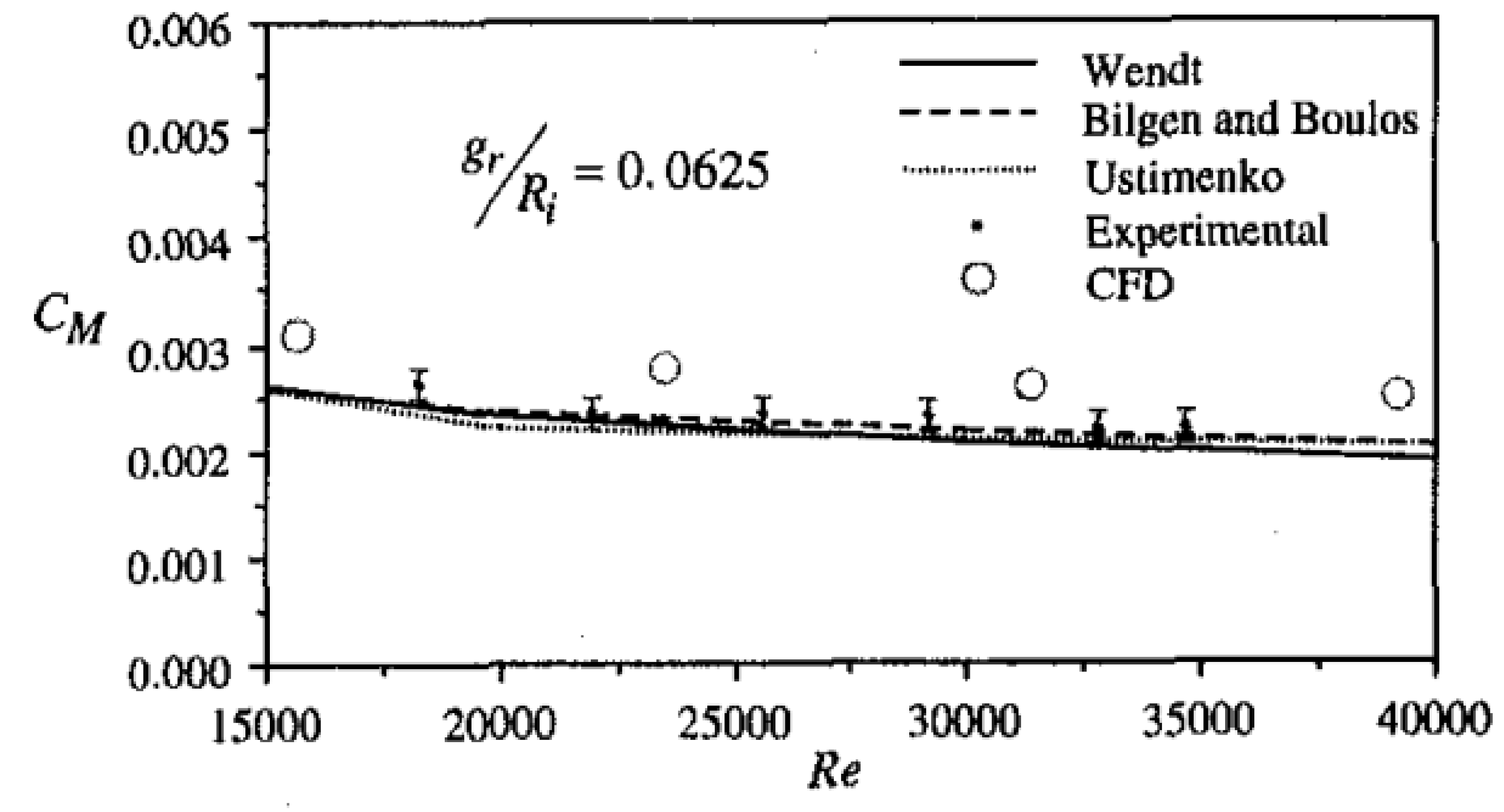

Fig. 8(b)

Fig. 8 Comparison of computed, measured and calculated moment coefficients: (a) $g_r/R = 0.0275$; (b) $g_r/R_i = 0.0625$

Wild, P. M., Djilali, N., & Vickers, G. W. (1996). Experimental and computational assessment of windage losses in rotating machinery.

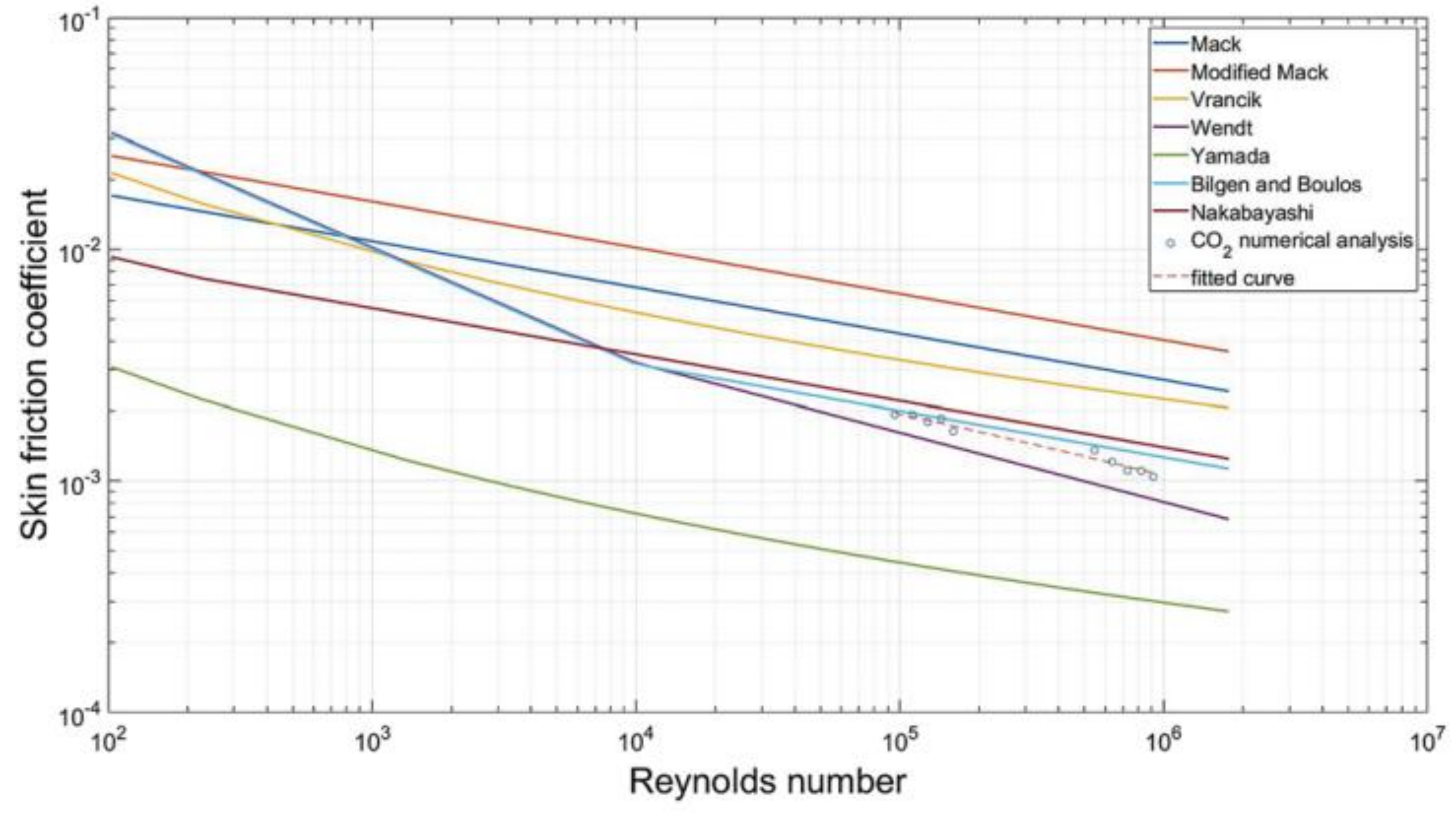

Fig. 5 C_f versus Re_r windage loss model comparison

Kim, D., Jeong, Y., Son, I. W., & Lee, J. I. (2023). Windage Loss Models for Enclosed Cylindrical Flows Under S-CO2 Condition. *Journal of Engineering for Gas Turbines and Power*

Secondary flow segments in TAC

- Across segments 1 through 11, the secondary flow receives heat due to viscous heating, and its density continuously changes.
- Since the density continuously changes, a linear regression approach cannot be adopted to determine the C_f and the exponents of ρ & ω.

$$W_{windage+disk} = \sum_{j=11} C_{f,j} \pi \rho_j^a \omega^b G_j \quad where\ G_j = \begin{bmatrix} R_{outer,j}^5 - R_{inner,j}^5\ (disk) \\ R_j^4 L_j\ (windage) \end{bmatrix}$$

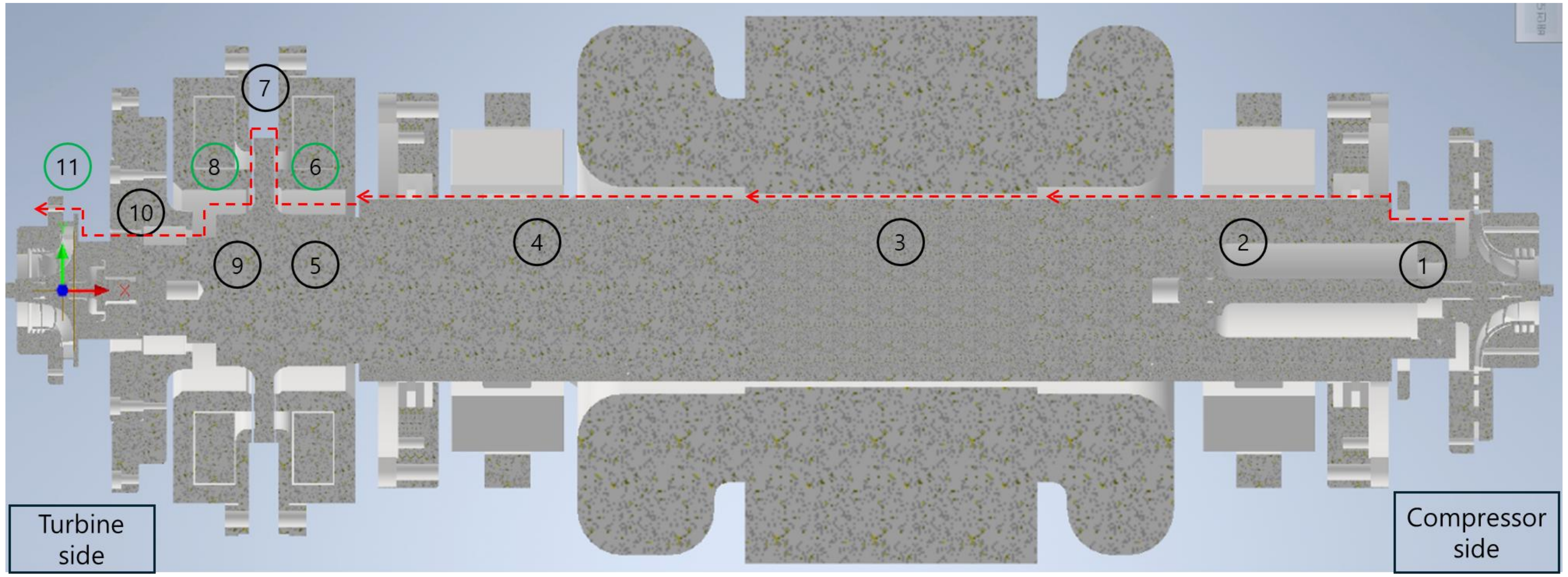

Segment	Radius (in mm)	Inner Radius (in mm) (disk friction)	Length (in mm) (windage)
1	22.35		21.1
2	30		117
3	30		94.8
4	30		127.2
5	25		28.4
6	50	25	
7	50		7
8	50	25	
8	25		16.3
10	16		45.1
11	25.8	16	

Data Filtering & Aggregation

- Rotor experimental data collected from all the experiment campaign of the KAIST-TAC.
- Data filtering condition as below;
  - $\omega_{min} = 0.4\omega_{design}$
  - $5\,\text{sec}\; steady\ state$
  - $P_{in} > P_{critical}, T_{in} > T_{critical}$
- Under this criterion, more than 100,000 data points would be generated, making subsequent matrix computations difficult. Therefore, a data aggregation step to group similar data was performed.
- Data aggregation criteria
  - $\text{Temperature} = 1\ \text{Kelvin}$
  - $\text{Pressure} = 10\ \text{kPa}$
  - $\text{Rotational speed}(\omega) = 10\ \text{RPM}$
- As a result, the calculations were carried out using 9,406 data points.
- Density histogram shows 250 to 500 kg/m^3 from these data points.

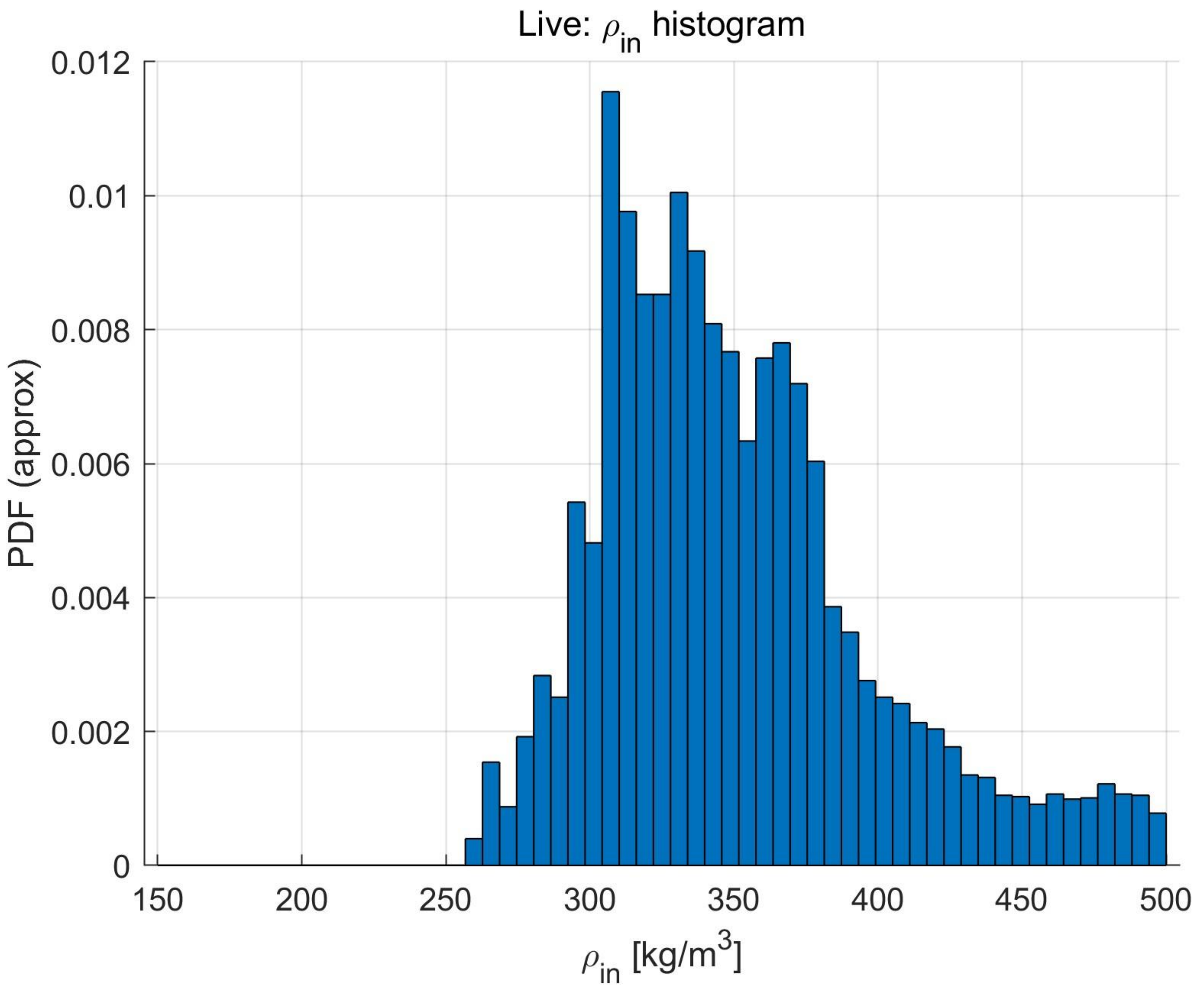

Calibration concept: parity target

- 1st station begins from compressor impeller outlet, and its state $(\rho_{1,i}, h_{1,i})$is predicted same as compressor diffuser outlet state with P, T measurements.
- As secondary flow flows 11 segments sequentially, $h_{2\sim 12,i}$ are calculated by disk and windage loss correlations stage by stage.
- Residual, r_i, is defined by difference between measurement($h_{tb\ inlet,i}$) and prediction($h_{12,i}$) to show the loss models appropriateness

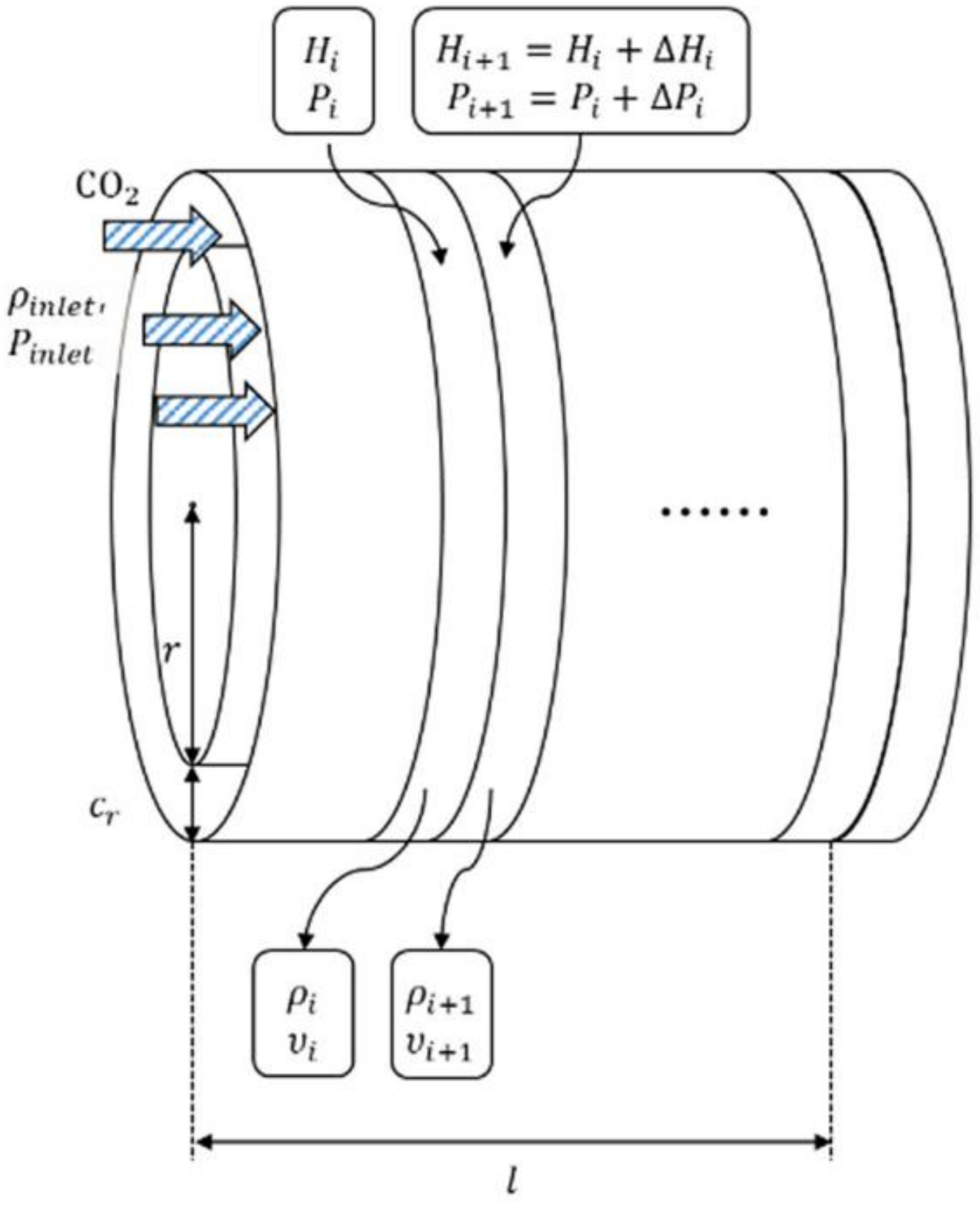

$$h_{12,i} = h_{1,i} + \Delta h_{loss,i}$$

$$\Delta h_{loss,i} = \sum_{j=11} C_{f,j} \pi \rho_j^a \omega^b G_j$$

$$where\ G_j = [\begin{matrix} R_{outer,j}^5 - R_{inner,j}^5\ (disk) \\ R_j^4 L_j\ (windage) \end{matrix}]$$

$$\underbrace{r_i}_{\text{residual}} = \underbrace{h_{12,i}}_{\text{prediction}} - \underbrace{h_{tb\ inlet,i}}_{\text{measurement}}$$

$$y_i = h_{tb\ inlet,i} - h_{1,i}$$

Original model result

- In most data points, predicted enthalpy at j=12 (h_{12}) exceed measured enthalpy (h_{turb}).
- It indicates that the original windage loss model is overpredicting compared to actual values.
- Plotting the results with an emphasis on density and rotational speed, it can be confirmed that density and rotational speed have an influence.
- More than 60% of the data points were estimated to be at least twice the target windage loss.
- Accordingly, it was confirmed that calibration of the windage loss model is necessary.

	Mean Absolute Error (kJ / kg)	Root Mean Square Error (kJ / kg)	Proportion (%) where, $\left\|\frac{r_i}{y_i}\right\| > 1.0$
Original model	**14.1**	**16.4**	**60.7**

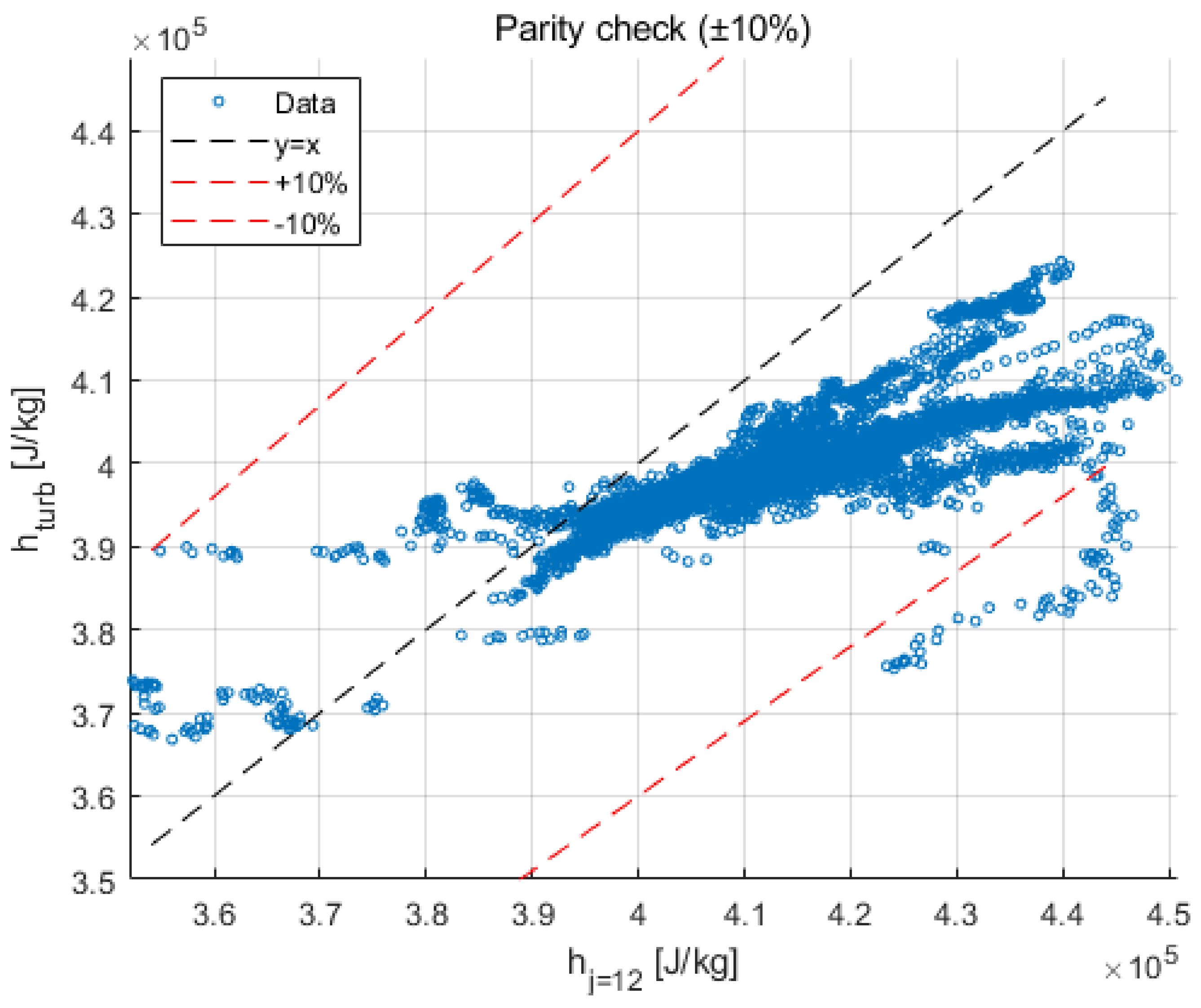

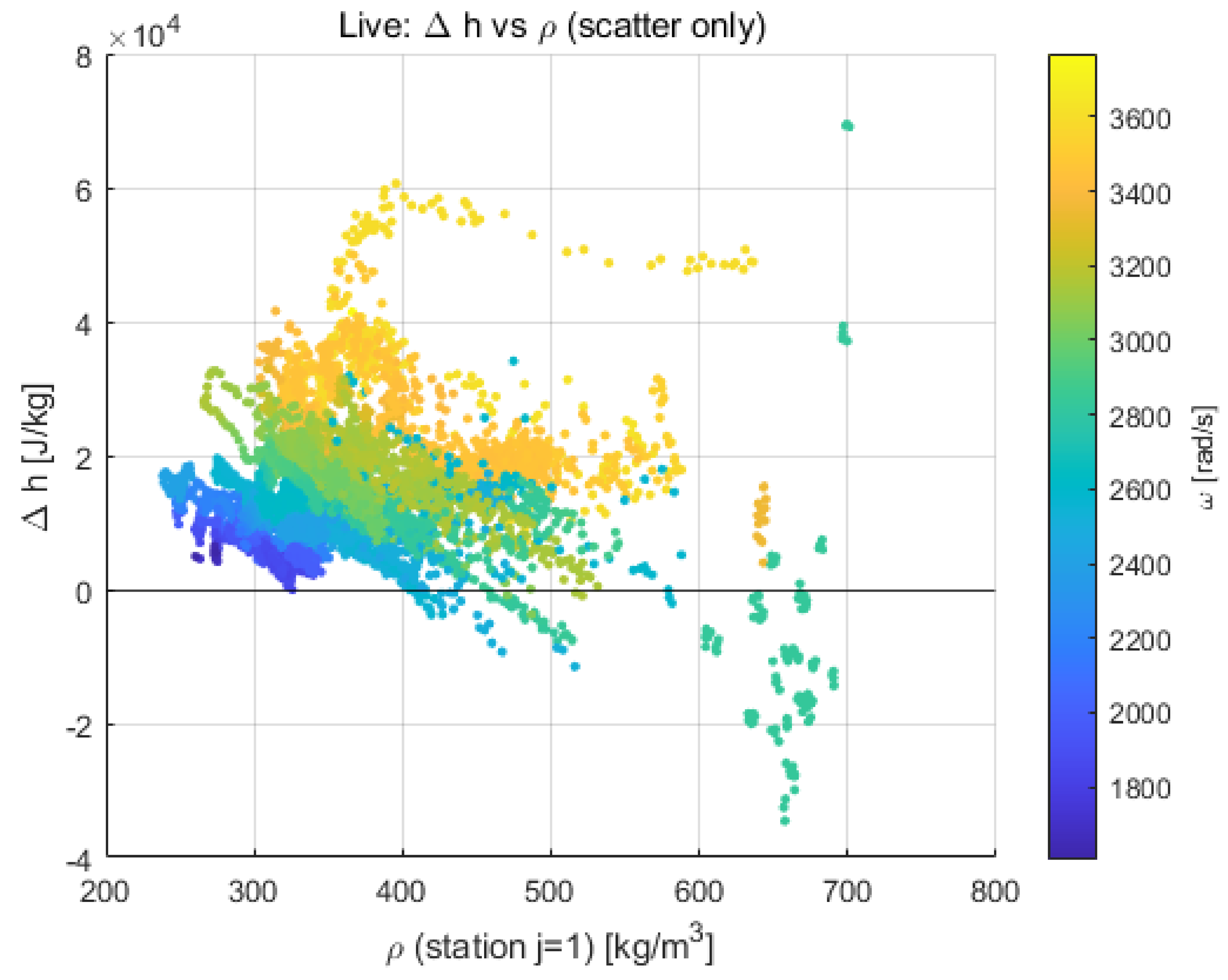

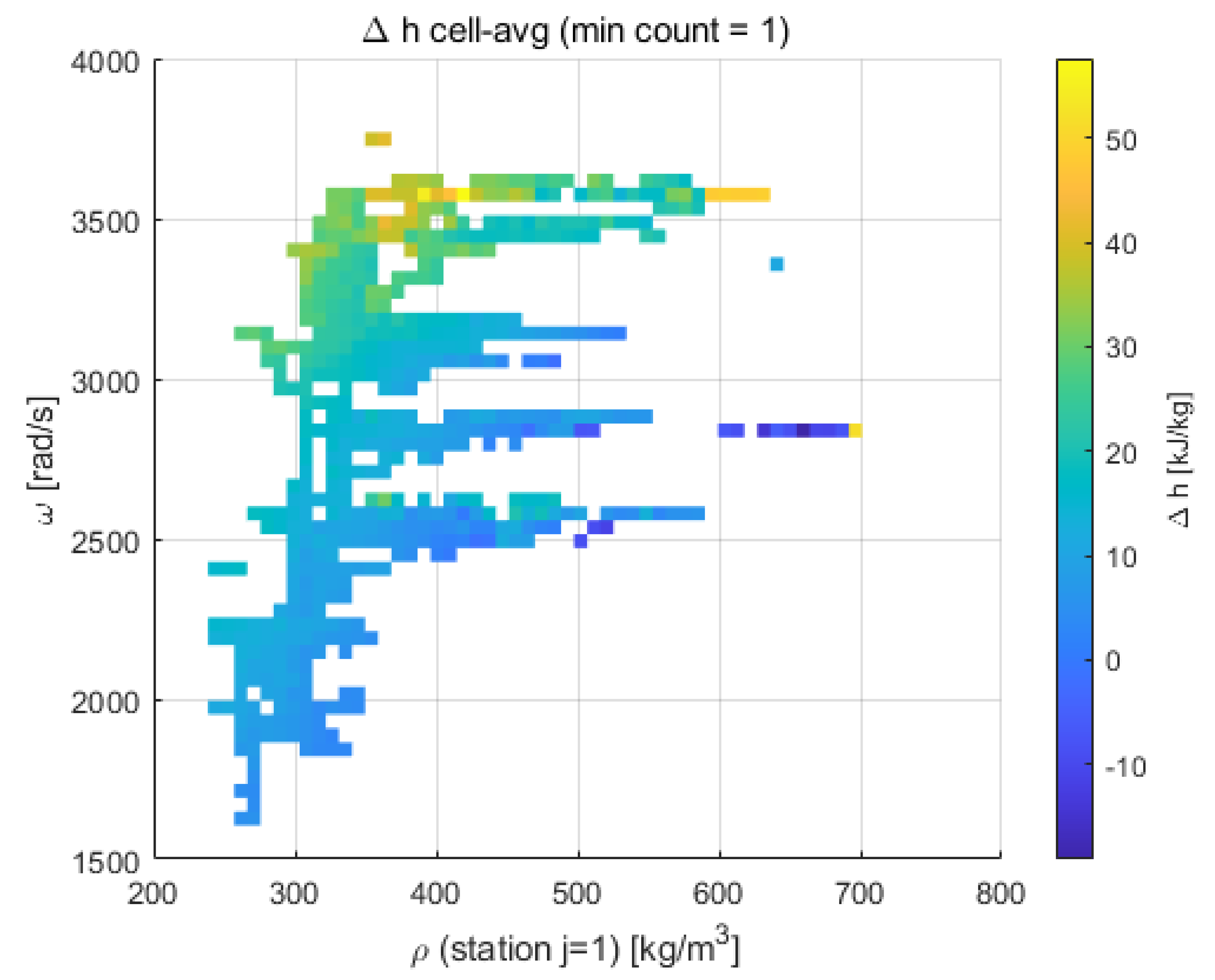

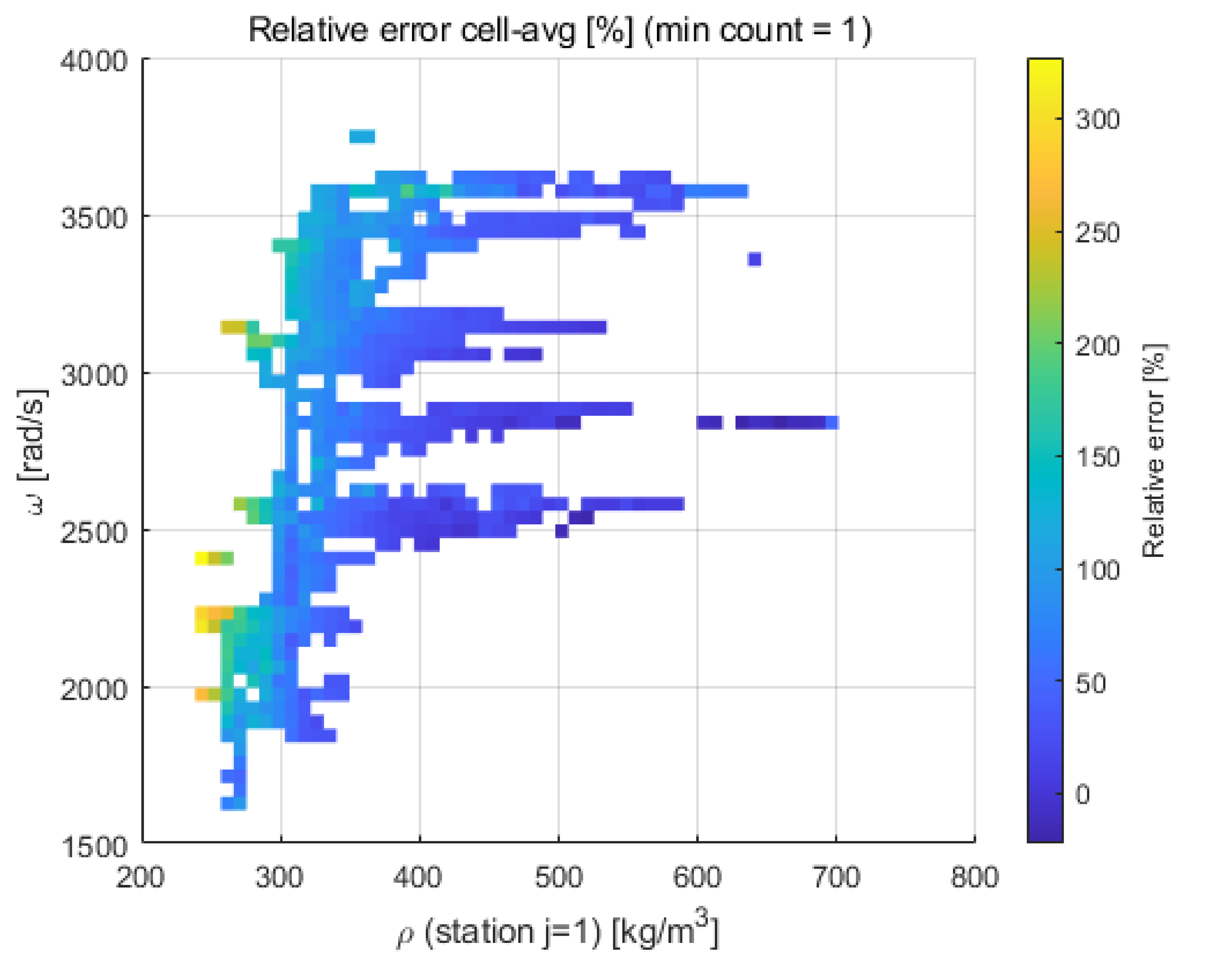

Closed form Coefficient Calibration

$w(a,b)$ & y & r $is\ (N,1)^{th}\ vector$

Target value

$$y_i = h_{tb\ inlet,i} - h_{1,i}$$

$$from\ W_{i,j}(a,b) = C_f G_j \rho_{i,j}^a \omega_i^b,$$

$$let\ w_{i,j}(a,b) = \frac{1}{\dot{m}} \sum_{j \in 1\sim 11} G_j \rho_{i,j}^a \omega_i^b$$

Residual

$$r_i(C,a,b) = Cw_i(a,b) - y_i$$

Objective function

$$S(C,a,b) = \frac{1}{2}\sum_{i \in S}\{r_i(C,a,b)\}^2 = \frac{1}{2}\|Cw(a,b) - y\|^2$$

Fixed a, b & $w^T y = y^T w$

$$2S(C,a,b) = (Cw - y)^T(Cw - y) = C^2(w^T w) - 2C(w^T y) + (y^T y)$$

$$\frac{dS}{dC} = C(w^T w) - (w^T y)$$

C* is optimized coefficient

$$\left.\frac{dS}{dC}\right|_{C^*} = C^*(w^T w) - (w^T y) = 0$$

$$\boldsymbol{C^* = \frac{w^T y}{w^T w}}$$

$and\ also,$

$$\left.\frac{dS}{dC}\right|_{C^*} = w^T(Cw - y) + (Cw^T - y^T)w$$

$$= w^T r + r^T w = 0$$

For (N,1)th vectors, $w^T r = r^T w$

$$\boldsymbol{r^T w = w^T r = 0}$$

C_f Calibration Result

$$W_{windage} = C_f \pi \rho R_j^4 \omega^3 L_j$$

$$C_f = 1.0 * 10^{-3} \ (set)$$

$$\downarrow$$

$$C_f = 3.91 * 10^{-4} \ (calibrated)$$

	Original model		Cf calibration model
Mean Error (kJ / kg)	**13.8**	86% →	**1.19**
Mean Absolute Error (kJ / kg)	**14.1**	66% →	**4.85**
Root Mean Square Error (kJ / kg)	**16.4**	56% →	**7.26**
Point Proportion (%) where, $\left\|\frac{r_i - y_i}{y_i}\right\| > 1.0$	**60.7**	78% →	**13.5**

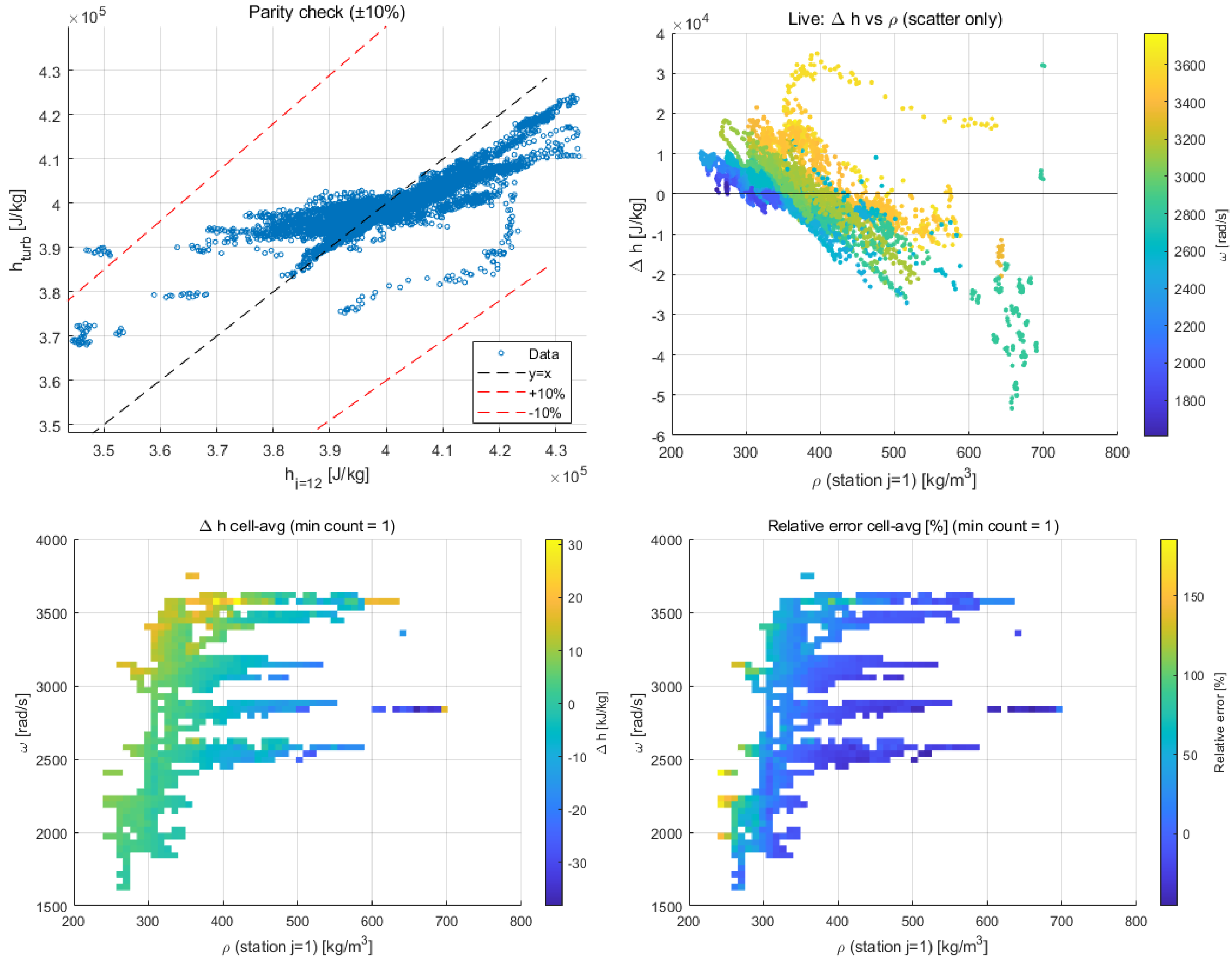

2 variable Newton-Gauss method

Objective function

$$S(C,a,b) = \frac{1}{2}\sum_{i\in S}\{r_i(C,a,b)\}^2 = \frac{1}{2}\|Cw(a,b) - y\|^2$$

Reduced Objective function

$$\tilde{S}(a,b) = S(C^*(a,b),a,b) = \frac{1}{2}\|r(a,b)\|^2 = \frac{1}{2}(r^T r)$$

Residual Residual form

$$r(a,b) = C^*(a,b)w(a,b) - y$$

Derivative residual of exponent

$$\frac{dr}{da} = \frac{dC^*}{da}w + C^*\frac{dw}{da}$$

Derivative objective func. of exponent

$$\frac{d\tilde{S}}{da} = r^T\frac{dr}{da} = \underbrace{\left(\frac{dC^*}{da}\right)r^T w}_{=0} + C^* r^T w_a = C^* r^T w_a$$

$$= C^* w_a^T r$$

Derivative of Objective function

$$g(a,b) = \nabla S(a,b) = \begin{bmatrix} d\tilde{S}/da \\ d\tilde{S}/db \end{bmatrix} = C^*\begin{bmatrix} w_a^T r \\ w_b^T r \end{bmatrix}$$

Hessian of Objective function

$$H(a,b) = \nabla^2\tilde{S}(a,b), \qquad \nabla^2\tilde{S}(a,b)\Big|_{C^*} = 0 \quad let\ \theta_k = [a_k, b_k]^T,$$

$$\tilde{S}(\theta_k + \Delta) \approx \tilde{S}(\theta_k) + g(\theta_k)^T\Delta + 1/2\Delta^T H(\theta_k)\Delta$$

$$since\ \frac{\partial\tilde{S}}{\partial\Delta} = 0, \qquad \frac{\partial}{\partial\Delta}\left(g^T\Delta + \frac{1}{2}\Delta^T H\Delta\right) = g + H\Delta = 0$$

Find Δa, Δb by

$$\begin{bmatrix} C^* w_a^T r + H_{aa}\Delta a + H_{ab}\Delta b \\ C^* w_b^T r + H_{ba}\Delta a + H_{bb}\Delta b \end{bmatrix} \approx \begin{bmatrix} C^* w_a^T r + {C^*}^2 w_a^T w_a \Delta a + {C^*}^2 w_a^T w_b \Delta b \\ C^* w_b^T r + {C^*}^2 w_b^T w_a \Delta a + {C^*}^2 w_b^T w_b \Delta b \end{bmatrix} = 0$$

C_f , exponent Calibration Result

$$W_{windage} = 1.0 * 10^{-3} \pi \rho R_j^4 \omega^3 L_j$$

$$\downarrow$$

$$W_{windage,new} = 8.7241 * 10^{-5} \left(\frac{\rho}{\rho_{ref}}\right)^{1.53} \left(\frac{\omega}{\omega_{ref}}\right)^{-0.91} \pi \rho R_j^4 \omega^3 L_j$$

	Original model		C_f calibration model	C_f, exponent calibration model
Mean Error (kJ / kg)	13.8	86% →	1.19	1.23
Mean Absolute Error (kJ / kg)	14.1	66% →	4.85	3.98
Root Mean Square Error (kJ / kg)	16.4	56% →	7.26	5.56
Point Proportion (%) where, $\left\lvert\frac{r_i - y_i}{y_i}\right\rvert > 1.0$	60.7	78% →	13.5	11.8

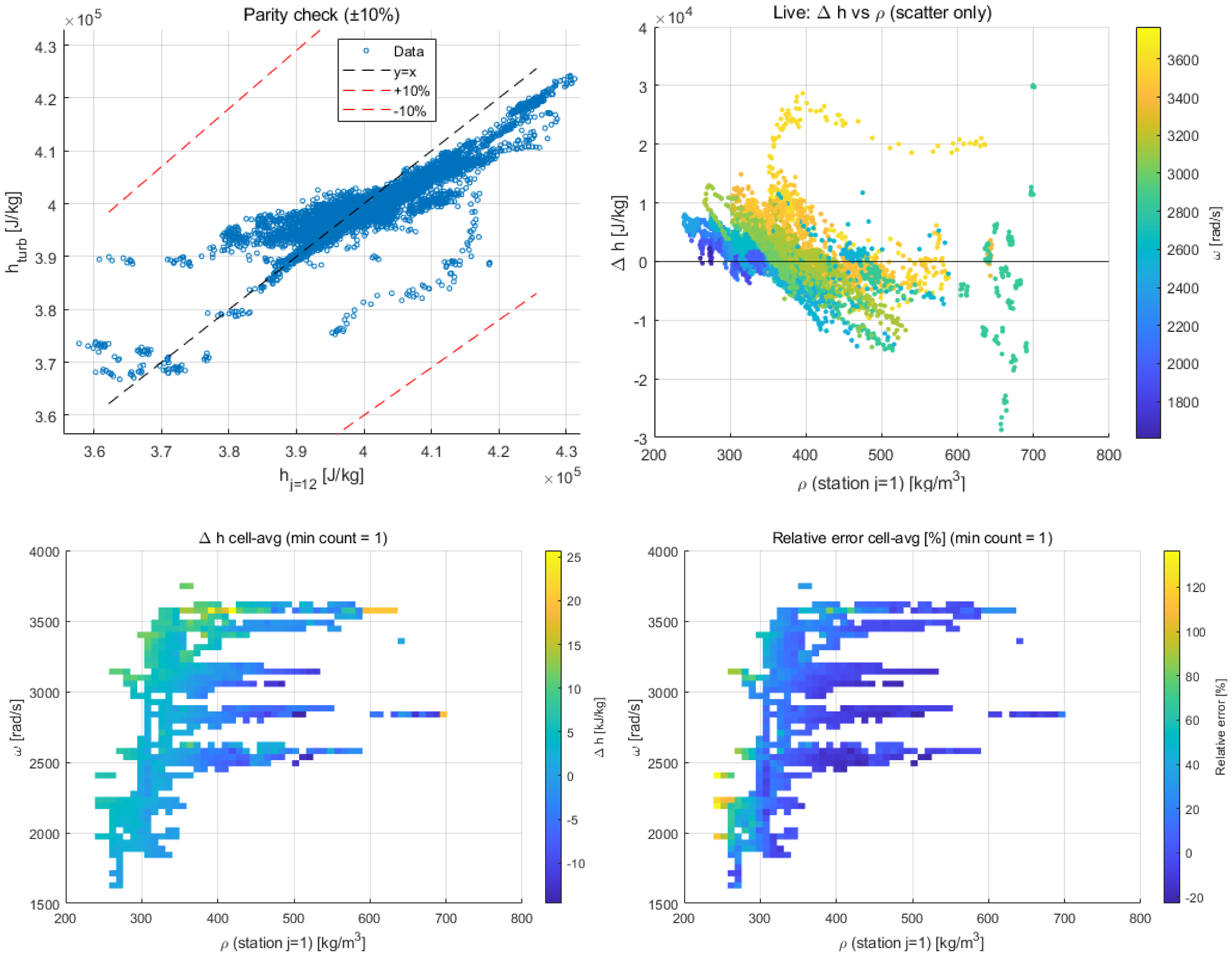

Original and Calibrated Correlations Results

- **Top row:** Parity plots compare predicted vs. reference enthalpy, and the y=x line is ideal.

- **Bottom row:** The error Δh is plotted against inlet density ρ and colored ω, revealing ρ-ω dependent bias in the baseline model.

- **After calibration:** The data cluster closer to y=x axis and Δh close to 0, indicating improved agreement and robustness across the operating envelope.

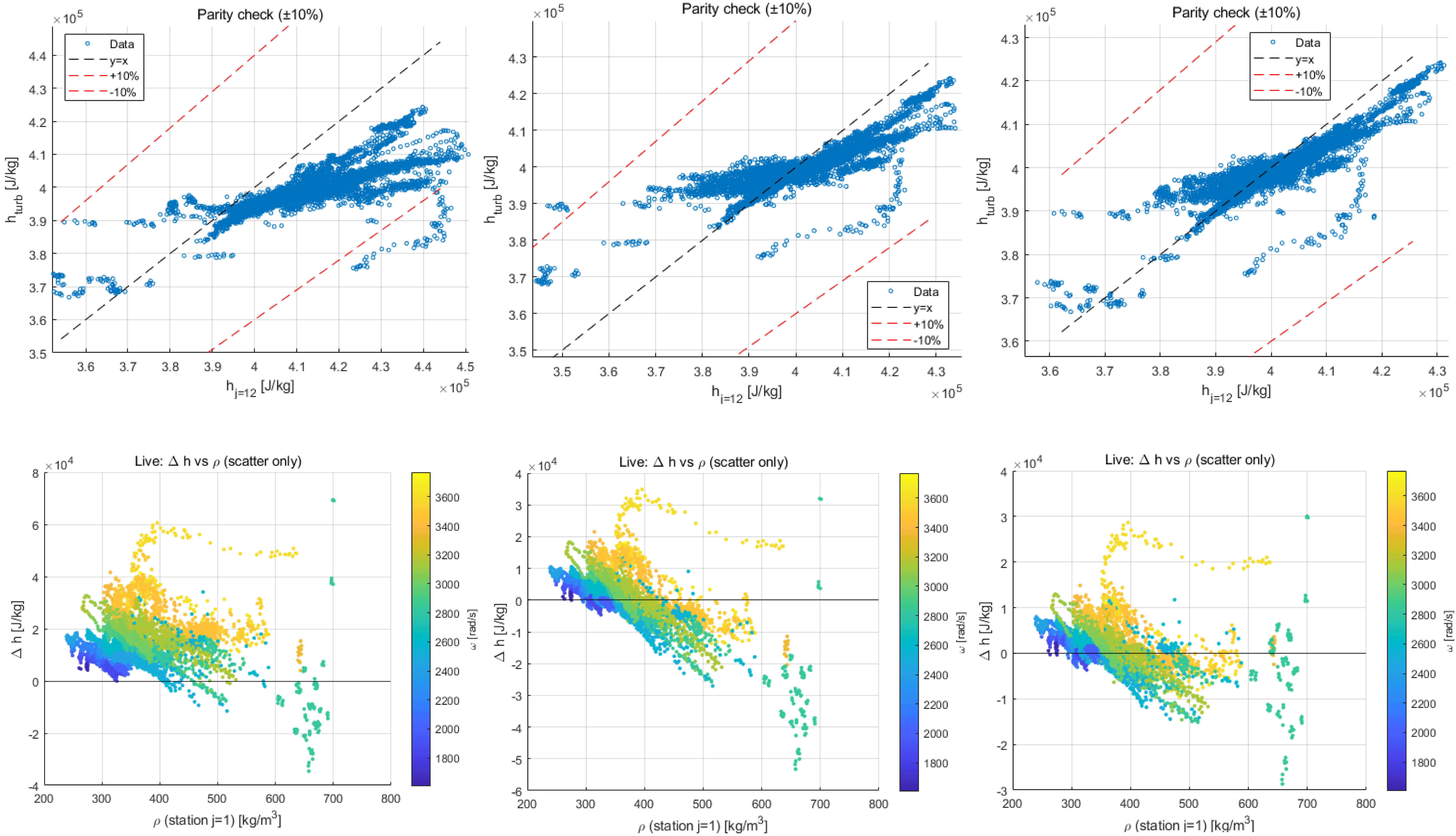

Conclusions

- **Motivation**: Identifying that the windage loss in the high density sCO_2 leakage path is substantially larger than initially predicted, critical for small scale sCO_2 turbomachinery shaft power.

- **Measurement constraint**: Along the rotor, disk friction and windage losses occur sequentially along the secondary flow. However, thermocouple is currently impractical due to narrow clearances.

- **Methodological challenge**: Conventional linear regression can't be utilized to calibrate the coefficients because the sequential heating causes continuous property (density) variation and its nonlinearity.

- **Calibration approach**: Using variable separation, the constant coefficient is obtained in closed form, while the two exponent coefficients are optimized via a least-squares objective function with the residual and Hessian-based updates for Δ(a, b).

- **Key outcome**: The calibrated correlations match the target enthalpy rise more accurately than the original model. It demonstrates that even a black-box-like secondary-flow windage loss in narrow sCO_2 clearances can be effectively inferred through a simple numerical calibration.

Thank you for listening !